Cooperative Voltage Control in AC Microgrids

Michele Cucuzzella, Sebastian Trip, Antonella Ferrara and Jacquelien Scherpen

***Abstract*— This paper proposes a novel control scheme based on the joint use of decentralized Sliding Mode (SM) control and distributed averaging control for cooperative voltage regulation in Alternate Current (AC) microgrids. The considered model of the microgrid includes several Distributed Generation Units (DGUs) interconnected through resistive-inductive power lines. In each DGU a Voltage Sourced Converter (VSC) supplies an unknown current load. The proposed control strategy consists of two different control schemes. A decentralized SM control scheme constrains the state of the microgrid on a suitable manifold where the q-component of the voltage of each DGU is equal to zero. On this manifold, the d-component of the control input is generated by distributed controllers aimed at sharing the d-component of the generated current and preserving the average of the microgrid voltages. Global convergence to a desired steady state is proven and simulation results confirm the effectiveness of the proposed solution.**

I. Introduction

Recently, due to the wide diffusion of Renewable Energy Sources (RES), power generation and distribution are rapidly changing towards sustainable and environmental friendly small-scale power systems known as *microgrids*. The emerging microgrids are clusters of Distributed Generation Units (DGUs), energy storage systems and loads, which are interconnected through power lines [1]. Voltage and frequency stability are the main control objectives in AC microgrids that work disconnected from the main grid, which would otherwise play the role of an infinite power source fixing voltage amplitude and frequency at the point of common coupling. However, the unpredictable power generation of RES and the unknown load dynamics require the design of robust and advanced control strategies, providing additionally a form of power sharing. For these reasons, in the recent years, microgrids have received much attention and are attracting growing interest within the control and electrical engineering communities.

A. Literature review and main contributions

Although there exits a vast amount of literature on the design of control schemes for AC microgrids (see e.g. [2] and the references therein), there are still some unresolved issues. For example, achieving *provably* a form of active and reactive power sharing in low voltage AC microgrids with inductive-resistive distribution lines is still lacking. Indeed, various approaches assume that the lines are purely inductive [3]–[6], which is often required to perform the stability analysis. However, this assumption is generally not valid in low voltage microgrids, where the line resistance is not negligible. On the other hand, for fairly general AC microgrid models, the focus has been on provably achieving only one objective, such as voltage regulation [7]–[9]. This paper provides some new results for AC microgrids that are mostly resistive, with a strong coupling between the active power generation and the voltage levels at the DGUs [10], [11]. Particularly, under the assumption of synchronization among the converters, we propose a distributed control scheme to regulate the average voltage in the network, while sharing generated currents associated to the active power generation fairly among the sources. We elaborate on two contributions below.

1) We consider voltage regulation for a three-phase AC microgrid in the dq-coordinate frame, including inductive-resistive lines. The q-component of the voltage at each DGU is controlled to zero to decouple the active and reactive power generation. This is achieved by a suitably designed third-order sliding mode control strategy [12], providing a continuous signal suitable for a Pulse Width Modulation (PWM) implementation. The d-component of the voltage is then controlled by a distributed integral control, sharing the d-component of the generated current and achieving an *average voltage regulation*, where the average of the voltage magnitudes at the DGUs is identical to the desired value.

2) We provide a provably stabilizing control scheme, where global convergence to a desired state is shown. Particularly, the combined use of sliding mode and distributed integral control appears to be powerful, enabling new perspectives on possible controller designs. Besides the theoretical convergence guarantees, a case study indicates that also the performance of the proposed control scheme is good.

II. AC Microgrid Model

In this work we consider a connected three-phase AC microgrid, consisting of n nodes, where every node corresponds to a Distributed Generation Unit (DGU) including a Voltage Sourced Converter (VSC) and a load*, which is assumed to be unknown. Note that such a network might be a result of reduction methods, such as Kron/Ward reduction [13]†. We make the following assumption (common for stability purposes) on the considered model [7]–[9]:

M. Cucuzzella, S. Trip and J. Scherpen are with the Jan C. Wilems Center for Systems and Control, ENTEG, Faculty of Science and Engineering, University of Groningen, Nijenborgh 4, 9747 AG Groningen, the Netherlands, (email: {m.cucuzzella, s.trip, j.m.a.scherpen}@rug.nl). A. Ferrara is with Dipartimento di Ingegneria Industriale e dell'Informazione, University of Pavia, via Ferrata 5, 27100 Pavia, Italy (e-mail: antonella.ferrara@unipv.it).

This work is supported by the EU Project 'MatchIT' (project number: 82203). *This is the final version of the accepted paper submitted for inclusion in the Proceedings of the IEEE Conference on Decision and Control, Miami Beach, FL, USA, Dec. 2018.*

*We consider constant current loads operating at nominal frequency.

†It is therefore important that possible control schemes are independent of the topology of the microgrid model.

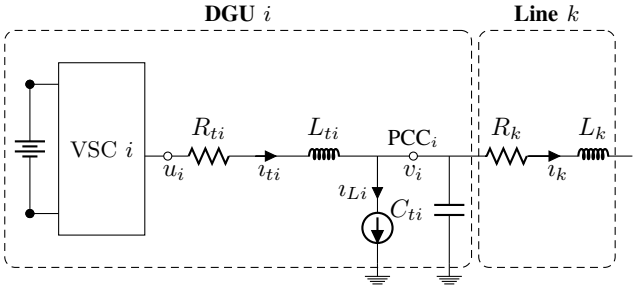

Fig. 1. Electrical single-line diagram of DGU i and line k of a typical islanded AC microgrid.

TABLE I
DESCRIPTION OF THE USED SYMBOLS

$\imath_t$	Generated current
v	Load voltage
$\imath$	Line current
R_t	Filter resistance
L_t	Filter inductance
C_t	Shunt capacitor
R	Line resistance
L	Line inductance
f_0	Microgrid nominal frequency
u	Control input
$\imath_L$	Unknown current demand

Assumption 1 (Operating conditions) *The microgrid is balanced and symmetric.*

The dynamics of phase a at the i-th node are then given by

$$\begin{aligned} C_{ti}\dot{v}_{ai} &= \imath_{tai} + \sum_{k\in\mathcal{E}_i} \imath_{ak} - \imath_{Lai} \\ L_{ti}\dot{\imath}_{tai} &= -R_{ti}\imath_{tai} - v_{ai} + u_{ai}, \end{aligned} \tag{1}$$

where $\mathcal{E}_i$ is the set of lines adjacent to node i. The remaining symbols are defined in Table I (see also Figure 1). The distribution lines are assumed to be resistive-inductive and consequently, the dynamics of phase a at the k-th line, connecting node i and node j, is given by

$$L_k\dot{\imath}_{ak} = v_{ai} - v_{aj} - R_k\imath_{ak}. \tag{2}$$

The dynamics of phase b and phase c are defined similarly. To obtain an overall model describing the microgrid, we represent its topology by an undirected graph $\mathcal{G} = (\mathcal{V}, \mathcal{E})$, with nodes $\mathcal{V} = \{1, ..., n\}$ and edges $\mathcal{E} = \{1, ..., m\}$. The network topology can then be represented by its corresponding incidence matrix $\mathcal{B} \in \mathbb{R}^{n\times m}$, which is obtained by labelling the ends of edge k arbitrarily with a $+$ and a $-$, and defining

$$\mathcal{B}_{ik} := \begin{cases} +1 & \text{if node } i \text{ is at the positive end of } k \\ -1 & \text{if node } i \text{ is at the negative end of } k \\ 0 & \text{otherwise .} \end{cases}$$

Next, we also define $v := (v_a^T, v_b^T, v_c^T)^T$. Vectors $\imath_t, \imath, \imath_L$ and u are defined similarly. The dynamic equations governing the network can now be expressed as

$$\begin{aligned} (\mathbb{I}_3 \otimes C_t)\dot{v} &= \imath_t + (\mathbb{I}_3 \otimes \mathcal{B})\imath - \imath_L \\ (\mathbb{I}_3 \otimes L_t)\dot{\imath}_t &= -(\mathbb{I}_3 \otimes R_t)\imath_t - v + u \\ (\mathbb{I}_3 \otimes L)\dot{\imath} &= -(\mathbb{I}_3 \otimes \mathcal{B}^T)v - (\mathbb{I}_3 \otimes R)\imath, \end{aligned} \tag{3}$$

where $\otimes$ denotes the Kronecker product and $\mathbb{I}_3 \in \mathbb{R}^{3\times3}$ denotes the identity matrix. Matrices C_t, L_t, $R_t \in \mathbb{R}^{n\times n}$ and $L, R \in \mathbb{R}^{m\times m}$ are diagonal and positive definite. Since in low voltage AC microgrids the lines are predominately resistive, there is a strong coupling between the active power and the voltage magnitude [10], [11]. Then, we aim to control the voltages by proper regulation of the active power, and regard the control of reactive power, which is strongly coupled to the frequency, to be outside of the scope of this paper. Following e.g. [7]–[9], [14], we assume that the frequency in the network is controlled in open-loop by equipping each VSC with an internal oscillator that provides the phase angle $\delta(t) = \int_{t_0}^{t} \omega_0 d\tau$, with $\omega_0 = 2\pi f_0$, f_0 being the nominal frequency of the microgrid, leading to the following assumption:

Assumption 2 (Clock synchronization) *All clocks of local controllers are synchronized*[‡].

Under Assumptions 1 and 2, the three-phase variables of system (3) can be transformed to the rotating dq-frame by the so-called Clarke's and Park's transformations [17]. As a result, system (3) can be equivalently represented as

$$\begin{aligned} C_t\dot{V}_d &= \omega_0 C_t V_q + I_{td} + \mathcal{B}I_d - I_{Ld} \\ C_t\dot{V}_q &= -\omega_0 C_t V_d + I_{tq} + \mathcal{B}I_q - I_{Lq} \\ L_t\dot{I}_{td} &= -V_d - R_t I_{td} + \omega_0 L_t I_{tq} + u_d \\ L_t\dot{I}_{tq} &= -V_q - \omega_0 L_t I_{td} - R_t I_{tq} + u_q \\ L\dot{I}_d &= -\mathcal{B}^T V_d - RI_d + \omega_0 LI_q \\ L\dot{I}_q &= -\mathcal{B}^T V_q - \omega_0 LI_d - RI_q. \end{aligned} \tag{4}$$

In the rotating dq-frame, the states of (4) represent the (real) component d and the (imaginary) component q of the corresponding three-phase signals, e.g. V_d and V_q are the dq-components of v, respectively.

Remark 1 (Additional load nodes) *Mutatis mutandis, the results derived in this work can also incorporate nodes $\mathcal{V}_L = \{1, ..., n_L\}$ representing constant impedance and constant current loads (ZI–loads), where the dynamic behaviour of load node $i \in \mathcal{V}_L$ is given by*

$$\begin{aligned} C_{ti}\dot{V}_{di} &= \omega_0 C_{ti} V_{qi} + \sum_{k\in\mathcal{E}_i} I_{dk} - I_{Ldi} - \frac{V_{di}}{R_{Li}} \\ C_{ti}\dot{V}_{qi} &= -\omega_0 C_{ti} V_{di} + \sum_{k\in\mathcal{E}_i} I_{qk} - I_{Lqi} - \frac{V_{qi}}{R_{Li}}, \end{aligned} \tag{5}$$

R_{Li} being the resistance of the constant impedance load. Since the required modification are fairly straightforward, we focus on system (4) *for the sake of exposition.*

[‡]In [14], a synchronization via GPS is proposed, achieving an accuracy higher than 1 µs. Moreover, currently available (low-cost) internal oscillators are characterized by an accuracy in the range of 20 ps–2 µs per year [15], [16].

III. Cooperative voltage regulation

In this section we formulate the considered control objective of cooperative voltage regulation. First we recall for the readers' convenience, the expressions for active power P_i and reactive power Q_i at a node, using the dq coordinates:

$$P_i = \frac{3}{2}(V_{di}I_{tdi}+V_{qi}I_{tqi}), \quad Q_i = \frac{3}{2}(V_{qi}I_{tdi}-V_{di}I_{tqi}). \quad (6)$$

As a first step it appears to be convenient to decouple the active and reactive power control, by requiring V_q to be regulated to zero. Consequently (6) becomes $P_i = \frac{3}{2}V_{di}I_{tdi}$, $Q_i = -\frac{3}{2}V_{di}I_{tqi}$, and one can notice that the active power P_i depends on the generated direct current I_{tdi}, whereas the reactive power Q_i does not. We make this decoupling explicit in the following objective:

Objective 1 (Active and reactive power decoupling)

$$\lim_{t\to\infty} V_q(t) = \overline{V}_q = \mathbf{0}. \quad (7)$$

When Objective 1 is achieved, for given I_{Ld}, I_{Lq} and constant inputs $\overline{u}_d$, $\overline{u}_q$, a steady state solution $(\overline{V}_d, \overline{V}_q = \mathbf{0}, \overline{I}_{td}, \overline{I}_{tq}, \overline{I}_d, \overline{I}_q)$ to system (4) satisfies

$$I_{Ld} - \overline{I}_{td} = \mathcal{B}\overline{I}_d \quad (8a)$$
$$I_{Lq} - \overline{I}_{tq} = -\omega_0 C_t \overline{V}_d + \mathcal{B}\overline{I}_q \quad (8b)$$
$$\overline{V}_d = -R_t\overline{I}_{td} + \omega_0 L_t \overline{I}_{tq} + \overline{u}_d \quad (8c)$$
$$0 = -\omega_0 L_t \overline{I}_{td} - R_t\overline{I}_{tq} + \overline{u}_q \quad (8d)$$
$$\overline{I}_d = -R^{-1}\mathcal{B}^T\overline{V}_d + \omega_0 R^{-1}L\overline{I}_q \quad (8e)$$
$$\overline{I}_q = -\omega_0 R^{-1}L\overline{I}_d \quad (8f)$$

From (8a) it follows[§] that the steady state value of the total generated direct current $\mathbb{1}^T\overline{I}_{td}$ is equal to the total current $\mathbb{1}^T I_{Ld}$ demanded by resistive loads. To avoid the overstressing of a source, we propose to share the total generated direct current fairly (proportionally to their capacity) among various sources:

Objective 2 (Direct current sharing)

$$\lim_{t\to\infty} I_{td}(t) = \overline{I}_{td} = W^{-1}\mathbb{1}i_t^*, \quad (9)$$

with $W = \mathrm{diag}(w_1, \ldots, w_n)$, $w_i > 0$, *for all* $i \in \mathcal{V}$ *and* $i_t^* \in \mathbb{R}$.

Here, the weights in W are related to the capacity of the DGUs, where a relatively large value of w_i corresponds to a relatively small generation capacity of DGU i. Indeed, the achievement of Objective 2 implies that at the steady state $w_i\overline{I}_{tdi} = w_j\overline{I}_{tdj}$ for all $i, j \in \mathcal{V}$. Furthermore, from (8) it follows that necessarily $i_t^* = \mathbb{1}^T I_{Ld}/\mathbb{1}^T W^{-1}\mathbb{1}$. Lastly, we consider voltage regulation and make the assumption that there exists a desired voltage magnitude at each DGU:

Assumption 3 (Desired voltages) *There exists a reference voltage magnitude* $|V_i^\star| = \sqrt{(V_{di}^\star)^2 + (V_{qi}^\star)^2}$ *at the PCC, for all* $i \in \mathcal{V}$.

[§]The incidence matrix $\mathcal{B}$, satisfies $\mathbb{1}^T\mathcal{B} = \mathbf{0}$, where $\mathbb{1} \in \mathbb{R}^n$ is the vector consisting of all ones.

Note that achieving Objective 1 implies that the desired voltage magnitude is completely described by the d-component of the voltage, i.e. $|V_i^\star| = V_{di}^\star$. For this reason, the voltage regulation objective will be formulated in terms of V_d. Due to Objective 2, some deviations from the desired voltage levels are needed. Indeed, from equations (8a), (8e) and (8f) it straightforwardly follows that the steady state voltage $\overline{V}_d$ satisfies $\mathcal{B}(\mathbb{I} + \omega_0^2 R^{-2}L^2)^{-1}R^{-1}\mathcal{B}^T\overline{V}_d = W^{-1}\mathbb{1}i_t^* - I_{Ld}$. This generally prohibits that the steady state voltage is identical to the desired value $V_d^\star$. However, there is still freedom to shift all the steady state direct voltages with the same constant value, since $\mathcal{B}^T\overline{V}_d = \mathcal{B}^T\left(\overline{V}_d + a\mathbb{1}\right)$, with $a \in \mathbb{R}$ any scalar. We formulate therefore the objective of *average voltage regulation*. Following the standard practise where the sources with the largest generation capacity determine the microgrid voltage, we select a weight of $1/w_i$ for all $i \in \mathcal{V}$:

Objective 3 (Average voltage regulation)

$$\lim_{t\to\infty} \mathbb{1}^T W^{-1}V_d(t) = \mathbb{1}^T W^{-1}\overline{V}_d = \mathbb{1}^T W^{-1}V_d^\star. \quad (10)$$

IV. The Proposed Solution

To design a control scheme achieving the objectives discussed in the previous section, we make the following assumption on the available microgrid parameters and measurements:

Assumption 4 (Available information) *The value of the filter resistance* R_{ti} *and inductance* L_{ti} *are known at converter* $i \in \mathcal{V}$. *Furthermore, the generated current* $\imath_{ti}$ *and the PCC voltage* v_i *are measured at converter* $i \in \mathcal{V}$.

The solution we propose in this section will consists of two separate components, controlling the inputs u_d and u_q. In the coming subsection, inspired by the distributed averaging controller for DC microgrids proposed in [18], [19], we design a distributed averaging controller generating u_d aiming at achieving Objectives 2 and 3. Thereafter, we design u_q in a decentralized fashion in order to achieve Objective 1.

A. Distributed averaging control

First, in order to achieve Objective 2 and Objective 3, we design a distributed controller at node $i \in \mathcal{V}$ of the form

$$\begin{aligned} T_{\theta i}\dot{\theta}_i &= -\sum_{j\in\mathcal{N}_i^c} \gamma_{ij}(w_i I_{tdi} - w_j I_{tdj}) \\ T_{\phi i}\dot{\phi}_i &= -\phi_i + I_{tdi} \\ u_{di} &= -K_i(I_{tdi} - \phi_i) + w_i \sum_{j\in\mathcal{N}_i^c} \gamma_{ij}(\theta_i - \theta_j) \\ &\quad + V_{di}^\star + R_{ti}I_{tdi} - \omega_0 L_{ti}I_{tqi}, \end{aligned} \quad (11)$$

with $T_{\theta i}, T_{\phi i}, K_i \in \mathbb{R}_{>0}$. The set $\mathcal{N}_i^c$ is the set of VSCs connected to VSC i via a communication network, with edge weights $\gamma_{ij} = \gamma_{ji} \in \mathbb{R}_{>0}$. Note that the controller is distributed as it prescribes the exchange of information on I_{td} and θ among neighboring nodes. Similar to the topology of the microgrid, the overall communication network is represented

by a connected and undirected graph $\mathcal{G}^c = (\mathcal{V}^c, \mathcal{E}^c)$, where $\mathcal{V}^c = \mathcal{V}$ and the edges, $\mathcal{E}^c = \{1, ..., m_c\}$, represent the communication links between the DGUs. The communication network topology is described by its corresponding incidence matrix $\mathcal{B}^c \in \mathbb{R}^{n \times m_c}$, which is defined similarly as $\mathcal{B}$. The overall control scheme can be compactly written for all $i \in \mathcal{V}$ as

$$
\begin{aligned}
T_\theta \dot{\theta} &= -\mathcal{L}^c W I_{td} && \text{(12a)}\\
T_\phi \dot{\phi} &= -\phi + I_{td} && \text{(12b)}\\
u_d &= -K(I_{td} - \phi) + W\mathcal{L}^c\theta \\
&\quad + V_d^\star + R_t I_{td} - \omega_0 L_t I_{tq}, && \text{(12c)}
\end{aligned}
$$

where $T_\theta, T_\phi, K \in \mathbb{R}^{n\times n}$ are positive definite diagonal matrices. Furthermore, $\mathcal{L}^c = \mathcal{B}^c\Gamma(\mathcal{B}^c)^T$ is the (weighted) Laplacian matrix associated to the communication network and $\Gamma \in \mathbb{R}^{m_c \times m_c}$ is a positive definite diagonal matrix describing the weights on the edges. Then, the closed-loop system of (4) interconnected with the distributed controller (12) is given by

$$
\begin{aligned}
C_t\dot{V}_d &= \omega_0 C_t V_q + I_{td} + \mathcal{B}I_d - I_{Ld}\\
C_t\dot{V}_q &= -\omega_0 C_t V_d + I_{tq} + \mathcal{B}I_q - I_{Lq}\\
L_t\dot{I}_{td} &= -V_d - K(I_{td} - \phi) + W\mathcal{L}^c\theta + V_d^\star\\
L_t\dot{I}_{tq} &= -V_q - \omega_0 L_t I_{td} - R_t I_{tq} + u_q\\
L\dot{I}_d &= -\mathcal{B}^T V_d - RI_d + \omega_0 L I_q\\
L\dot{I}_q &= -\mathcal{B}^T V_q - \omega_0 L I_d - RI_q\\
T_\theta\dot{\theta} &= -\mathcal{L}^c W I_{td}\\
T_\phi\dot{\phi} &= -\phi + I_{td},
\end{aligned}
\qquad (13)
$$

where u_q will be designed in a decentralized way in the next subsection to achieve Objective 1.

B. Decentralized sliding mode control

Now, in order to achieve also Objective 1, we propose decentralized third-order Sliding Mode (SM) controllers to steer, in a finite time T_r, the state of system (13) to the following desired manifold:

$$
\{(V_d, V_q, I_{td}, I_{tq}, I_d, I_q, \theta, \phi) : V_q = \dot{V}_q = \mathbf{0}\}. \qquad (14)
$$

Consequently, we consider the following sliding function:

$$
\sigma(V_q) = V_q. \qquad (15)
$$

Regarding (15) as the output function of system (4), it appears that the relative degree[¶] is two. This implies that a second-order SM controller can be *naturally* applied in order to make the state of the controlled system reach, in a finite time, the manifold (14). However, this approach generates a discontinuous control signal and, as a consequence, the IGBTs switching frequency cannot be a-priori fixed and the power losses could be high. Then, to obtain a continuous control input permitting a Pulse Width Modulation (PWM) implementation, we adopt the procedure suggested e.g. in [20] and [21] for controlling boost and buck converters, respectively. This procedure consists of integrating the discontinuous control input generated by a SM controller, i.e.,

$$
\begin{aligned}
C_t\dot{V}_d &= \omega_0 C_t V_q + I_{td} + \mathcal{B}I_d - I_{Ld}\\
C_t\dot{V}_q &= -\omega_0 C_t V_d + I_{tq} + \mathcal{B}I_q - I_{Lq}\\
L_t\dot{I}_{td} &= -V_d - K(I_{td} - \phi) + W\mathcal{L}^c\theta + V_d^\star\\
L_t\dot{I}_{tq} &= -V_q - \omega_0 L_t I_{td} - R_t I_{tq} + u_q\\
L\dot{I}_d &= -\mathcal{B}^T V_d - RI_d + \omega_0 L I_q\\
L\dot{I}_q &= -\mathcal{B}^T V_q - \omega_0 L I_d - RI_q\\
T_\theta\dot{\theta} &= -\mathcal{L}^c W I_{td}\\
T_\phi\dot{\phi} &= -\phi + I_{td}\\
\dot{u}_q &= \mu,
\end{aligned}
\qquad (16)
$$

where μ is the new (discontinuous) control input. This procedure indeed ensures that the input signal to the VSC, $u_q(t) = \int_0^t \mu(\tau)d\tau$, is continuous. Since the system relative degree with respect to the new control input μ is now equal to three, it is needed to apply a third-order SM control. To do this, we define the auxiliary variables $\xi_1 = \sigma$, $\xi_2 = \dot{\sigma}$ and $\xi_3 = \ddot{\sigma}$. Then, the dynamics of the corresponding auxiliary system are given by

$$
\begin{aligned}
\dot{\xi}_1 &= \xi_2\\
\dot{\xi}_2 &= \xi_3\\
\dot{\xi}_3 &= \beta + B\mu\\
\dot{u}_q &= \mu.
\end{aligned}
\qquad (17)
$$

Bearing in mind hat $\dot{\xi}_3 = \sigma^{(3)} = \beta + B\mu$, the expressions for the mapping $\beta \in \mathbb{R}^n$ and matrix $B \in \mathbb{R}^{n\times n}$ can be straightforwardly obtained from (15) by taking the third derivative of σ with respect to time, yielding for the latter[‖] $B = L_t^{-1}C_t^{-1}$. Note that, β and B are not completely known because of possible model uncertainty and unavailable measurements (see Assumption 4). Then, as usual in classic SM control theory [22], to permit the controller design, the following assumption is made on the boundedness of β and B:

Assumption 5 (Bounded uncertainty) *β_i and B_{ii} in (17) have known bounds, i.e.,*

$$
\begin{aligned}
|\beta_i| &\le \beta_i^{\max} && \forall i \in \mathcal{V}\\
0 < B_i^{\min} &\le B_{ii} \le B_i^{\max} && \forall i \in \mathcal{V},
\end{aligned}
\qquad (18)
$$

$\beta_i^{\max}, B_i^{\min}$ and $B_i^{\max}$ being positive constants.

Then, the 3SM control law proposed in [12] can be used to steer ξ_{1i}, ξ_{2i} and ξ_{3i}, $i \in \mathcal{V}$, to zero in a finite time, implying that the state of system (4) are constrained on the desired manifold (14) (see [12] for details about the control law).

V. Stability Analysis

In this section we first show that the states of (16) are constrained, after a finite time, to the desired manifold (14), achieving Objective 1. Thereafter, we prove that the solutions to (16), once the sliding manifold is attained, converge to a constant point, achieving also Objectives 2 and 3.

[¶] The relative degree is the minimum order ρ of the time derivative $\sigma_i^{(\rho)}, i \in \mathcal{V}$, of the sliding function associated with the i-th node in which the control $u_{qi}, i \in \mathcal{V}$ explicitly appears.

[‖] The expression for β is rather long and is omitted.

Lemma 1 (Achieving Objective 1) *Let Assumptions 1–5 hold. Given the sliding function* (15)*, the solutions to system* (16)*, controlled by the sliding mode control algorithm proposed in [12], converge in a finite time T_r to the manifold* (14)*.*

The proof directly follows from [23] and [12].

For the analysis of system (16), when the solutions are constrained to the sliding manifold, it is convenient to exploit the so-called system order reduction property, typical of sliding mode control methodology [24].

Lemma 2 (Equivalent reduced order system) *Let Assumptions 1–5 hold. For all $t \geq T_r$, the dynamics of the controlled system* (16) *are given by the following equivalent system of reduced order:*

$$\begin{aligned} C_t\dot{V}_d &= I_{td} + \mathcal{B}I_d - I_{Ld} \\ L_t\dot{I}_{td} &= -V_d - K(I_{td} - \phi) + W\mathcal{L}^c\theta + V_d^\star \\ L\dot{I}_d &= -\mathcal{B}^T V_d - RI_d + \omega_0 LI_q \\ L\dot{I}_q &= -\omega_0 LI_d - RI_q \\ T_\theta\dot{\theta} &= -\mathcal{L}^c W I_{td} \\ T_\phi\dot{\phi} &= -\phi + I_{td}, \end{aligned} \tag{19}$$

together with the following algebraic relations:

$$V_q = \mathbf{0} \tag{20}$$

$$I_{tq} = \omega_0 C_t V_d - \mathcal{B}I_q + I_{Lq}. \tag{21}$$

Lemma 2 can be straightforwardly proved by exploiting the result of Lemma 1, i.e., $V_q(t) = \dot{V}_q(t) = \mathbf{0}$ for all $t \geq T_r$.

Theorem 1 (Main result) *Let Assumptions 1–5 hold. Consider system* (16)*, controlled by the sliding mode control algorithm proposed in [12]. The solutions to the controlled system converge asymptotically to a steady steady ($\overline{V}_d, \overline{V}_q = \mathbf{0}, \overline{I}_{td}, \overline{I}_{tq}, \overline{I}_d, \overline{I}_q, \overline{\theta}, \overline{\phi}$), achieving power decoupling (Objective 1), direct current sharing (Objective 2) and average voltage regulation (Objective 3).*

The proof follows from evaluating the quadratic incremental storage function $\mathcal{S} = \frac{1}{2}(V_d - \overline{V}_d)^T C_t (V_d - \overline{V}_d) + \frac{1}{2}(I_{td} - \overline{I}_{td})^T L_t (I_{td} - \overline{I}_{td}) + \frac{1}{2}(I_d - \overline{I}_d)^T L (I_d - \overline{I}_d) + \frac{1}{2}(I_q - \overline{I}_q)^T L (I_q - \overline{I}_q) + \frac{1}{2}(\theta - \overline{\theta})^T T_\theta (\theta - \overline{\theta}) + \frac{1}{2}(\phi - \overline{\phi})^T T_\phi K (\phi - \overline{\phi})$, along the solutions to (19), and applying LaSalle's invariance principle.

VI. Simulation Results

In this section, we test in simulation the proposed control strategy described in Section IV. We consider an AC microgrid with nominal frequency $f_0 = 60\,\text{Hz}$, composed of 4 DGUs in a ring topology as shown in Figure 2, where also the communication network is depicted. The adopted microgrid parameters are reported in Tables II and III, and the weights associated with the communication links are $\gamma_{12} = \gamma_{23} = \gamma_{34} = 1 \times 10^2$. In the distributed controller (12), we select $T_\theta = \mathbb{I}_4$, $T_\phi = 1 \times 10^{-3}\ \mathbb{I}_4$, and $K = 5\ \mathbb{I}_4$,

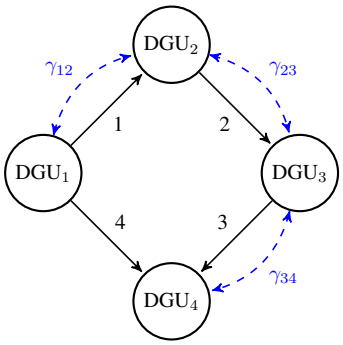

Fig. 2. Scheme of the considered microgrid composed of 4 DGus. The arrows indicate the positive direction of the currents through the power network. The dashed lines represent the communication network.

TABLE II
MICROGRID PARAMETERS AND CURRENT DEMAND

DGU		1	2	3	4
R_t	(mΩ)	40.2	38.7	34.6	31.8
L_t	(mH)	9.5	9.2	8.7	8.3
C_t	(μF)	62.86	62.86	62.86	62.86
w_i	–	0.4^{-1}	0.2^{-1}	0.15^{-1}	0.25^{-1}
$V_d^\star$	(V)	$120\sqrt{2}$	$120\sqrt{2}$	$120\sqrt{2}$	$120\sqrt{2}$
$V_q^\star$	(V)	0	0	0	0
$I_{Ld}(0)$	(A)	30.0	15.0	30.0	26.0
$I_{Lq}(0)$	(A)	−20.0	−15.0	−10.0	−18.0
ΔI_{Ld}	(A)	10.0	7.0	−10.0	5.0

TABLE III
LINE PARAMETERS

Line		1	2	3	4
R	(Ω)	0.25	0.27	0.24	0.26
L	(μH)	1.2	1.3	1.8	2.1

$\mathbb{I}_4 \in \mathbb{R}^{4\times4}$ being the identity matrix, while the amplitude of the sliding mode controller proposed in [12] is equal to 5×10^3 for all the DGUs. Consider that at the initial time instant the system is at steady state with current demand $I_{Ld}(0), I_{Lq}(0)$. Then, at the time instant $t = 1\,\text{s}$, there is a variation ΔI_{Ld} (see Table II) at the loads. Figures 3 and 4 show that the d-axis voltage at the PCC of each DGU is regulated in order to achieve proportional direct current sharing (Objective 2) while guaranteeing that at steady state the weighted average voltage of the microgrid (denoted by $V_{d,av}$) is equal to the weighted average of voltage references (Objective 3). Moreover, from the bottom of Figure 3 we conclude that sliding mode controllers keep the q-component of the voltage at each PCC equal to zero (Objective 1).

VII. Conclusions

In this paper, a novel control scheme based on the combained use of decentralized Sliding Mode (SM) control and distributed averaging control is proposed for cooperative voltage regulation in AC microgrids. After constraining the state of the controlled microgrid on a suitable manifold, global convergence to a desired steady state is proven independently

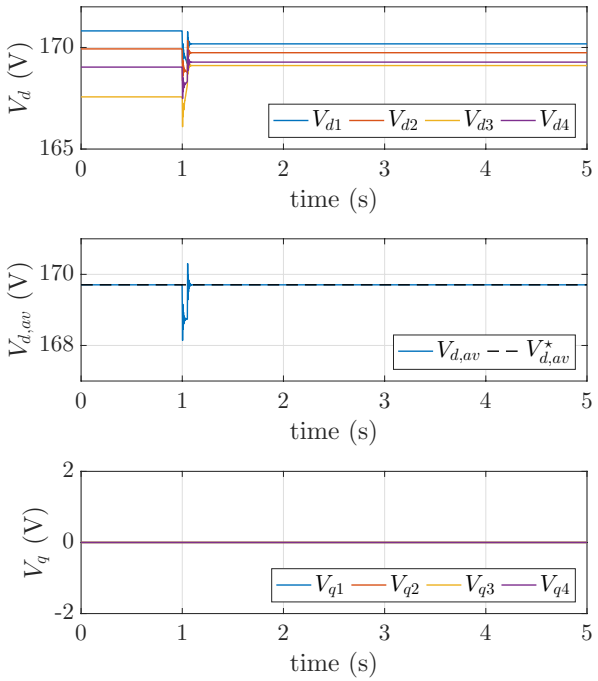

Fig. 3. From the top: d-component of the voltage at the PCC of each DGU; weighted average value of the d-component of the voltage at the PCC of each DGU; q-component of the voltage at the PCC of each DGU.

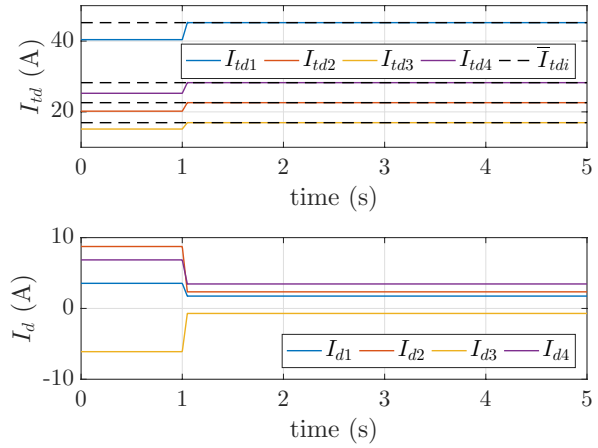

Fig. 4. From the top: d-component of the generated currents together with the corresponding values (dashed lines) that correspond to (proportional) direct current sharing for $t > 1$; d-component of the line currents.

of the initial conditions of the physical system and the controller state. Interesting future research includes extensions towards incorporating reactive power sharing by controlling the system frequency.

REFERENCES

[1] R. Lasseter and P. Paigi, "Microgrid: a conceptual solution," in *Proc. 35th IEEE Power Electron. Specialists Conf.*, vol. 6, Aachen, Germany, June 2004, pp. 4285–4290.

[2] J. M. Guerrero, M. Chandorkar, T. L. Lee, and P. C. Loh, "Advanced control architectures for intelligent microgrids–Part I: Decentralized and hierarchical control," *IEEE Transactions on Industrial Electronics*, vol. 60, no. 4, pp. 1254–1262, Apr. 2013.

[3] S. Trip, M. Bürger, and C. De Persis, "An internal model approach to frequency regulation in inverter-based microgrids with time-varying voltages," in *Proc. of the 53rd IEEE Conference on Decision and Control (CDC)*, Dec. 2014, pp. 223–228.

[4] J. Schiffer, T. Seel, J. Raisch, and T. Sezi, "Voltage stability and reactive power sharing in inverter-based microgrids with consensus-based distributed voltage control," *IEEE Transactions on Control Systems Technology*, vol. 24, no. 1, pp. 96–109, Jan. 2016.

[5] C. De Persis and N. Monshizadeh, "Bregman storage functions for microgrid control," *IEEE Transactions on Automatic Control*, vol. 63, no. 1, pp. 53–68, Jan. 2018.

[6] J. W. Simpson-Porco, F. Dörfler, and F. Bullo, "Synchronization and power sharing for droop-controlled inverters in islanded microgrids," *Automatica*, vol. 49, no. 9, pp. 2603–2611, 2013.

[7] M. Babazadeh and H. Karimi, "A robust two-degree-of-freedom control strategy for an islanded microgrid," *IEEE Transactions on Power Delivery*, vol. 28, no. 3, pp. 1339–1347, July 2013.

[8] M. S. Sadabadi, Q. Shafiee, and A. Karimi, "Plug-and-play voltage stabilization in inverter-interfaced microgrids via a robust control strategy," *IEEE Transactions on Control Systems Technology*, vol. 25, no. 3, pp. 781–791, May 2017.

[9] M. Cucuzzella, G. P. Incremona, and A. Ferrara, "Decentralized sliding mode control of islanded ac microgrids with arbitrary topology," *IEEE Transactions on Industrial Electronics*, vol. 64, no. 8, pp. 6706–6713, Aug. 2017.

[10] J. M. Guerrero, J. Matas, L. G. de Vicuna, M. Castilla, and J. Miret, "Decentralized control for parallel operation of distributed generation inverters using resistive output impedance," *IEEE Transactions on Industrial Electronics*, vol. 54, no. 2, pp. 994–1004, Apr. 2007.

[11] M. S. Golsorkhi, M. Savaghebi, D. D. C. Lu, J. M. Guerrero, and J. C. Vasquez, "A GPS-based control framework for accurate current sharing and power quality improvement in microgrids," *IEEE Transactions on Power Electronics*, vol. 32, no. 7, pp. 5675–5687, July 2017.

[12] F. Dinuzzo and A. Ferrara, "Higher order sliding mode controllers with optimal reaching," *IEEE Trans. Automat. Control*, vol. 54, no. 9, pp. 2126 –2136, Sept. 2009.

[13] F. Dörfler and F. Bullo, "Kron reduction of graphs with applications to electrical networks," *IEEE Transactions on Circuits and Systems I: Regular Papers*, vol. 60, no. 1, pp. 150–163, Jan 2013.

[14] A. H. Etemadi, E. J. Davison, and R. Iravani, "A decentralized robust control strategy for multi-der microgrids–Part I: Fundamental concepts," *IEEE Transactions on Power Delivery*, vol. 27, no. 4, pp. 1843–1853, Oct. 2012.

[15] A. G. Phadke and J. S. Thorp, *Synchronized phasor measurements and their applications*. Springer, 2017, vol. 1.

[16] J. R. Vig, "Quartz crystal resonators and oscillators for frequency control and timing applications. A tutorial," *NASA STI/Recon Technical Report N*, vol. 95, 1994.

[17] R. H. Park, "Two-reaction theory of synchronous machines - Generalized method of analysis - Part I," *Trans. American Instit. Electr. Eng.*, vol. 48, no. 3, pp. 716–727, 1929.

[18] S. Trip, M. Cucuzzella, X. Cheng, and J. Scherpen, "Distributed averaging control for voltage regulation and current sharing in DC microgrids," *IEEE Control Systems Letters*, vol. 3, no. 1, pp. 174–179, Jan. 2019.

[19] S. Trip, R. Han, M. Cucuzzella, X. Cheng, J. Scherpen, and J. Guerrero, "Distributed averaging control for voltage regulation and current sharing in DC microgrids: Modelling and experimental validation," in *7th IFAC Workshop on Distributed Estimation and Control in Networked Systems*, Groningen, the Netherlands, Aug. 2018.

[20] M. Cucuzzella, R. Lazzari, S. Trip, S. Rosti, C. Sandroni, and A. Ferrara, "Sliding mode voltage control of boost converters in DC microgrids," *Control Engineering Practice*, vol. 73, pp. 161–170, 2018.

[21] M. Cucuzzella, S. Trip, C. De Persis, X. Cheng, A. Ferrara, and A. van der Schaft, "A robust consensus algorithm for current sharing and voltage regulation in DC microgrids," *IEEE Transactions on Control Systems Technology*.

[22] V. I. Utkin, *Sliding Modes in Optimization and Control Problems*. New York: Springer Verlag, 1992.

[23] A. Levant, "Higher-order sliding modes, differentiation and output-feedback control," *Int. J. Control*, vol. 76, no. 9-10, pp. 924–941, Jan. 2003.

[24] C. Edwards and S. K. Spurgen, *Sliding Mode Control: Theory and Applications*. London, UK: Taylor and Francis, 1998.